PROCEEDINGS, Nineteenth Workshop on Geothermal Reservoir Engineering
Stanford University, Stanford, California, January 18-20, 1994
SGP-TR-147

AN INVERSE PROBLEM SOLUTION TO THE FLOW OF TRACERS IN NATURALLY FRACTURED RESERVOIRS

JETZABETH RAMÍREZ S., FERNANDO SAMANIEGO V., FERNANDO RODRÍGUEZ, AND JESÚS RIVERA R.

UNIVERSIDAD NACIONAL AUTÓNOMA DE MÉXICO
FACULTAD DE INGENIERÍA, 04510 MÉXICO, D.F.

ABSTRACT

This paper presents a solution for the inverse problem to the flow of tracers in naturally fractured reservoirs. The models considered include linear flow in vertical fractures, radial flow in horizontal fractures, and cubic block matrix-fracture geometry. The Rosenbrock method for nonlinear regression used in this study, allowed the estimation of up to six parameters for the cubic block matrix fracture geometry. The nonlinear regression for the three cases was carefully tested against syntetical tracer concentration responses affected by random noise, with the objective of simulating as close as possible step injection field data. Results were obtained within 95 percent confidence limits. The sensitivity of the inverse problem solution on the main parameters that describe this flow problem was investigated. The main features of the nonlinear regression program used in this study are also discussed. The procedure of this study can be applied to interpret tracer tests in naturally fractured reservoirs, allowing the estimation of fracture and matrix parameters of practical interest (longitudinal fracture dispersivity α, matrix porosity ϕ_2, fracture half-width w, matrix block size d, matrix diffusion coefficient D_2 and the adsorption constant k_d). The methodology of this work offers a practical alternative for tracer flow tests interpretation to other techniques.

INTRODUCTION

Most of the geothermal reservoirs currently under exploitation are found in naturally fractured formations. The behavior of these reservoirs is quite different from that of "homogeneous"-conventional-reservoirs. The complex matrix-fracture interaction of these systems makes their characterization a challenging task. Among the different tools currently available to accomplish this endeavor, tracer test interpretation is taking an ever increasing role. These interwell tracer tests have significantly contributed to the better understanding of the fluid flow in these systems. Radioactive and chemical tracers have been used for many years in groundwater hydrology to analyze the movement of water through porous formations, but their use in geothermal reservoir engineering is more recent (Jensen, 1983).

It has been recognized, as already stated, that tracer test interpretation, in addition to well-to-well pressure transient tests (Brigham and Abbaszadeh-Dehgani, 1987), is a very important contribution towards accomplishing the characterization of naturally fractured reservoirs. As concluded by these authors, these two testing techniques are complementary, not competing.

There are several papers that discuss the flow of tracers in naturally fractured reservoirs. For a review of the recent work the papers of Ramírez et al. (1990, 1991, 1992) may be consulted. Most of these studies deal with the direct problem (i.e., predicting the tracer response behavior from the knowledge of pertinent reservoir and tracer parameters). Methods for solving the inverse problem (i.e., estimating reservoir and tracer parameters from the interpretation of the tracer response), are much less numerous than solutions to the direct problem. This situation gets worst when dealing with naturally fractured reservoirs.

Fossum and Horne (1982) used the model of Horne and Rodríguez (1983), that accounts for dispersion during fluid flow through the fractures, to analyze tracer return profiles for the Wairakei geothermal field.

Jensen (1983) presented the application of a double porosity model, in a nonlinear least-squares procedure of curve fitting of tracer concentration responses. Fossum (1984) presented an application of a reformulated two dimensional double porosity model, using the same nonlinear least-squares procedure used by Jensen (1983). This model represented the fractured medium by a mobile region, in which convection, diffusion, and adsorption are allowed, and an immobile region in which only diffusion and adsorption are allowed. Other authors (Shinta and Kazemi, 1993), have recently considered the application of a two dimensional and two phase model to interpret an actual field test.

The purpose of this study is to present a solution for the inverse problem to the flow of tracers in naturally fractured reservoirs. The models considered include linear flow in vertical fractures, radial flow in horizontal fractures, and cubic block matrix-fracture geometry. The Rosenbrock method (1960) for nonlinear regression used in this study allowed the estimation of up to six parameters for the cubic block matrix-fracture geometry.

MATHEMATICAL MODELS

Models considered in this study are shown in Figs. 1 to 4. The naturally fractured medium, Fig. 1, is represented by means of Figs. 2 to 4, which correspond to the flow ge-

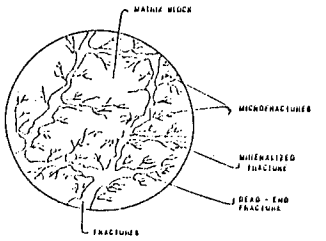

Fig. 1 Naturally fractured reservoir

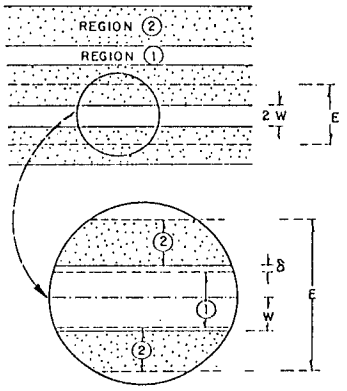

Fig. 2 Vertical fractures - linear flow - model

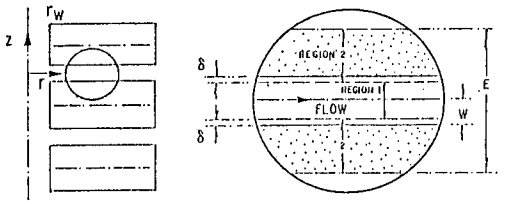

Fig. 3 Radial flow - horizontal fractures - model

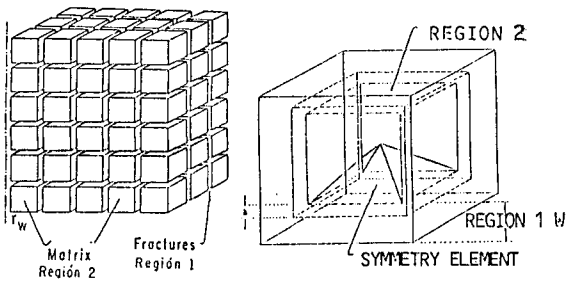

Fig. 4 Cubic matrix proposed model for representation of the flow of a tracer in a naturally fractured medium

ometries commonly present in these formations. Idealized models of naturally fractured reservoirs used to describe linear flow (vertical fractures), and radial flow (horizontal fractures) shown in Figs. 2 and 3, represent the fractured medium by means of a system of equally spaced parallel fractures, alternated with matrix blocks. Fig. 4 shows the ideal representation for the case of radial flow considering cubic matrix-fracture geometry, where the fractured medium is represented by means of a system of identical cubic blocks separated by an orthogonal network of fractures.

The system shown in these figures consists of two regions: 1) a mobile region constituted by the fracture network and 2) a stagnant or immobile region, constituted by the matrix blocks. This type of visualization of the problem has been used in previous works (Jensen, 1983; Ramírez et al., 1990, 1991, 1992). It is considered that these regions are interconnected by means of a thin layer of fluid, contained within the immobile region, which controls the mass transfer by diffusion between both regions.

The main assumptions considered in the three models are the following:
1. Constant density for species "A".
2. No velocity component in direction perpendicular to flow.
3. In the mobile region, the concentration gradient in the transverse flow direction is considered negligible.
4. The volume of the mobile region remains constant.
5. Adsorption takes place by means of a first order chemical reaction.
6. The mass transfer between the fracture and matrix systems is controlled by a fluid layer of infinitesimal thickness, δ, located at the interface between matrix blocks and surrounding fractures.
7. Tracer transport takes place by means of the following mechanims:
Mobile region (fractures): Difussion + Convection.
Stagnant region (Matrix blocks and dead-end fractures): Difussion + Adsorption.

The main difference between the linear and radial models is, that in the first case the velocity is constant, while for the radial cases, the velocity depends on the radial distance and therefore, the dispersion coefficient, D_r, is also a function of this radial distance. For the cases of radial flow under constant rate injection, the velocity is defined as:

$$v_r = \frac{a}{r} \tag{1}$$

where:

$$a = \frac{q}{2\pi h \phi_1} \tag{2}$$

where h is the reservoir thickness and ϕ_1 is the fracture porosity.

The solutions for the flow problems of vertical fractures (Ramírez et al., 1990), for the horizontal fractures (Ramírez et al., 1991), and for the cubic block matrix-fracture geometry (Ramírez and Samaniego, 1992), derived using the

Laplace tranform method, result for the case of linear flow in an analytic solution of the integral type and for the cases of radial flow, in a solution in Laplace space in terms of Airy functions. The solutions for the case of continuous tracer injection for the three models are as follows:

Linear Flow

$$C_{D1}(x_D,t_D) = \frac{1}{\sqrt{\pi}} exp\left(\frac{x_D P_{e1}}{2}\right) \int_0^{\infty} \frac{1}{(\tau'')^2} \cdot$$

$$exp\left[-\left(\frac{1}{\tau''}-1\right)^2 - \frac{P_{e1}x_D^2}{4\left(\frac{1}{\tau''}-1\right)^2}\left(\frac{P_{e1}}{4}+\gamma\right)\right] \cdot$$

$$\{F_1 + F_2\} U\left(t_D - \frac{P_{e1}x_D^2}{4\left(\frac{1}{\tau''}-1\right)^2}\right) d\tau'' \qquad (3)$$

where:

$$F_1 = \{exp(-A_1)\, erfc\{B_1 - C_1\}\} \qquad (4)$$

and

$$F_2 = \{exp(A_1)\, erfc\{B_1 + C_1\}\} \qquad (5)$$

where:

$$A_1 = \frac{x_D^2 P_{e1}\alpha}{4\left(\frac{1}{\tau''}-1\right)^2}\sqrt{\gamma} \qquad (6)$$

$$B_1 = \frac{x_D^2 P_{e1}\alpha}{8\left(\frac{1}{\tau''}-1\right)^2\sqrt{t_D - \frac{P_{e1}x_D}{4\left(\frac{1}{\tau''}-1\right)^2}}} \qquad (7)$$

and

$$C_1 = \sqrt{\gamma\left(t_D - \frac{P_{e1}x_D^2}{4\left(\frac{1}{\tau''}-1\right)^2}\right)} \qquad (8)$$

Radial Flow

Laplace space solutions to both horizontal fractures and cubic block-matrix fracture geometry cases, may be written in the following general form:

$$\overline{C}_{D1}(r_D,s) = \frac{1}{s} exp\left(\frac{Y-Y_0}{2}\right) \frac{A_i\left(\xi_r^{1/3}Y\right)}{A_i\left(\xi_r^{1/3}Y_0\right)} \qquad (9)$$

where:

$$Y = r_D + \frac{1}{4\xi_r} \qquad (10)$$

$$Y_0 = r_{D0} + \frac{1}{4\xi_r} \qquad (11)$$

The variable ξ_r depends on the geometry of the matrix-fracture system. For the layered matrix-fracture geometry, it is given as follows:

$$\xi_r = s + \gamma + \frac{D_{D2}}{z_{D0}}\beta_r . tanh\left\{4\beta_r\left(\frac{E_D}{2} - z_{D0}\right)\right\} \qquad (12)$$

and for tho cubic block matrix-fracture geometry:

$$\xi_r = s + \gamma + \varepsilon\left\{\beta_r\, coth\left(z_{D0}\,\beta_r\right) - \frac{1}{z_{D0}}\right\} \qquad (13)$$

where:

$$\varepsilon = \frac{6}{d_D}\frac{\phi_2}{\phi_1} D_{D2} \qquad (14)$$

$$\beta_r = \sqrt{\frac{s+\gamma}{RD_{D2}}} \qquad (15)$$

The integral of Eq. 3 was numerically integrated using the algorithm of O'Hara and Smith (1969). The solution for the radial flow models in real space was obtained using the algorithm of Crump (1976) as numerical invertor, and the Airy functions were computed according to Abramowitz and Stegun (1970).

A solution for the finite step injection case may be obtained through the use of Eqs. 3 and 9 and the principle of superposition.

In some tests, the tracer is injected for a short period and are referred to as"spike" injection tests (Walkup, 1984). It has been stated (Walkup and Horne, 1985; Walkup, 1984), that the solution for the spike injection test can be derived through the time derivative of the continuous solution.

OPTIMIZATION ALGORITHM

Optimization of the model parameters is accomplished using a nonlinear least-squares method of curve fitting. The objective function to be minimized is given by Eq. 16:

$$F(\alpha_1,\alpha_2,...,\alpha_j) = \sum_{i=1}^{N}[C(t_i) - C^*(t_i,\alpha_1,\alpha_2,...,\alpha_j)]^2 \qquad (16)$$

where:

$C(t_i)$	= measured tracer concentrations
$C(t_i,\alpha_j)$	= calculated tracer concentrations
α_j	= matching parameters
t	= time
N	= number of data points

It must be kept in mind that the reservoir-tracer parameters that could be estimated through the interpretation of a

tracer test, depend on the model used for this purpose. In this study the number of matching parameters used were 2, 5, and 2, 4 and 6, for the vertical (linear flow) fractures, horizontal (radial flow) fractures and cubic-block matrix fracture geometry, respectively.

The algorithm used to minimize the objective function given by Eq. 16 was that of Rosenbrock (1960). This is a direct search strategy method, where the direction of search and step lengths are fixed heuristically, or through a specific scheme, rather than through and optimal mathematical way (Fuentes, 1993). The main attraction of direct search methods rests on their proved simplicity and practicality.

The computer program used in this study to minimize the objective function given by Eq. 16 consists of a main program and four functions: a) The objective function; b) Function CX for the estimation of the matching parameters α_j; c) Function CG for the lower restrictions set on the α_j parameters; and d) Function CH for the upper restrictions of the α_j paramters. This optimization procedure does not limit the number of parameters to be matched, neither the type of restrictions. The required partial derivatives with respect to the matching parameters are calculated numerically; for example for the parameters α_1:

$$\frac{\partial F}{\partial \alpha_1} = \frac{F[\alpha_1 + \Delta\alpha_1, \alpha_2, ..., \alpha_j] - F[\alpha_1, \alpha_2, ..., \alpha_j]}{\Delta\alpha_1} \tag{17}$$

where $\Delta\alpha_1$ is a small differential increment.

This procedure requires an initial estimation for the matching parameters, and for the length of the optimization step, e, used in the solution of this problem.

For the initialization of this process, the objective function given by Eq. 16 is first evaluated with the initial data. Next, the objective function is evaluated with the result of incrementing the initial estimate by the optimization step e. If the function F decreases, we are moving in the right direction and the step e is multiplied by $\alpha_R(\alpha_R > 1)$. On the other hand, if F increases the step e is multiplied by - $\beta_R(0 \leq \beta_R \leq 1)$, and the direction of search is reversed. This procedure is followed for all the matching parameters. After each function evaluation, a check is made to determine whether the constraints are verified and boundary zones are not violated. The restrictions for the matching parameters were fixed based on the range of variation of the physical parameters reported in the literature (Grisak and Pickens, 1981; Weber and Baker, 1981; Hensel, 1981), as shown in Table 1.

DISCUSSION OF RESULTS

The results of this section are synthetic, generated for the injection of the radioactive tritium tracer in naturally fractured reservoirs. The tracer responses were computed by means of solutions given by Eqs. 3 and 9, in addition to Eqs. 12 and 13. As mentioned, the range of the data used for the generation of these results is presented in Table 1.

TABLE 1 RANGE OF THE PARAMETERS USED IN THIS STUDY (Partially taken from Pickens and Grisak, 1981; Weber and Baker, 1981; Hensel, 1989)

Injection rate,	$10 \leq$	$w, ton/hr$	≤ 300
Radial distance,	$200 \leq$	r, m	≤ 1000
Formation thick.,	$4.11 \leq$	h, m	≤ 100
Fracture width,	$.0001 \leq$	$, m$	≤ 0.01
Block size,	$2.05 \leq$	d, m	≤ 25
Fracture disper.,	$0.5 \leq$	α, m	≤ 400
Matrix porosity,	$0.01 \leq$	ϕ_2,frac.	≤ 0.35
Matrix diff coef,	1E-12$\leq$	$D_2, m^2/D$	$\leq$ 1.38E-5
Adsorption const,	$.5 \leq$	R,dimens.	≤ 1

With the purpose of simulating as close as possible real field conditions, random noise was introduced to the calculated tracer responses. The white noise consisted of a sorted non correlated sequence of numbers a_i, with a normal distribution with mean equal to zero and variance σ_a^2(Davis, 1973). The method used is based on the residual analysis (Montgomery, 1984), that considers that the independent random errors have a normal distribution, with mean equal to zero and variance equal to 1. The expresion used is given by Eq. 18:

$$C_{Di} = C_{Di} + a_i \tag{18}$$

where C_{Di} is either the tracer concentration at time t_i or that computed with Eqs. 3 and 9, a_i is the random error and C_{Di} is the concentration that simulates field data conditions.

This section presents results for conditions of finite step injection, for the three cases already mentioned. It is important to notice that for the case of vertical fractures only one fracture is considered; thus, due to the difference in pore volume between this case and the radial systems, smaller injection times were used in the linear example. Results presented are divided in two main groups. First the inverse problem is solved for "good data", which means synthetic data without noise. This is considered useful as a preliminary test of the capability of the optimization algorithm. Second, the algorithm is applied, as already mentioned, in a final test to noisy data. For the minimization of the objective function given by Eq. 16, a set of 34 data points was used.

Results of this study were generated for fixed values of the physical parameters that fall in the ranges presented in Table 1, included in Table 2. The values of column 2 of this table were taken from Jensen (1984). The exception is the value of fracture dispersivity α, which was considered in accordance to the finding of Pickens and Grisak (1981), stating that dispersivity is a function of the mean travel distance. The injection rate is considered in this linear case through the definition of the Peclet number for the

fractured region P_{e1}. In other words, we choose a fixed value of this parameter for each simulation, for these cases equal to 5. For this linear case the thickness corresponds to the horizontal thickness E of the repetitive element shown in Fig.2 (Ramírez et al., 1990), which has been shown by these authors that for practical purposes does not importantly affect the results. This assumption is considered in Eq. 3.

TABLE 2 DATA USED FOR THE TRACER RESPONSE EXAMPLES OF THIS STUDY

	Linear	Radial
Injection rate, $q\ m^3/D$	–	2400
Distance, L or $r\ m$	210	250
Formation thick., $h\ m$	–	4.11
Fracture width, $w\ m$	$1.8E-4$	$1.0E-4$
Block size, $d\ m$	–	2.05
Fracture disper., $\alpha\ m$	21	25
Matrix porosity, ϕ_2	0.01	0.01
Matrix diff coef, $D_2\ m^2/D$	$1.E-8$	$1.38E-5$
Adsorption const, k_d	1	1
Velocity, $v_L\ m/D$	909.6	–
Radioactive decay const.,$\lambda\ 1/D$	–	$1.534E-4$

As a starting point, Fig. 5 presents results for the linear flow of a chemical tracer in a vertical fractures case, for a finite step injection time t_D=0.85. The matching dimensionless parameters used are the Peclet number for the mobile or fractured region P_{eL} and the α parameter, which combines the parameters of the immobile region. The precision used to obtain these results was 1×10^5, yielding an optimized objective function of 1.02×10^5, with matching parameters reported in Table 3.

TABLE 3 LINEAR FLOW

	Fig. 5 "Good Data"		Fig. 6 "Noisy Data"	
Real parameters	Initial	Matched	Initial	Matched
$\alpha_1 = P_{e1} = 10$	5	10.07	8	10.26
$\alpha_2 = \alpha = .0027$	.004	.0045	.0015	.0098

Fig. 6 shows the results of Fig. 5 after being altered to include random noise. In this graph and those to follow, the continuous curve represents the match, and the individual symbols the data to be matched. The discontinuous curves, as indicated, correspond to the 95% confidence intervals. The precision used to obtain these results was 1×10^5, yielding an optimized objective function of 1.23×10^2, with matching parameters reported in Table 3. We can observe that despite the dispersion of the noisy data, most of it fall within the confidence interval bandwith. Table 3 shows a comparion of matched results of Figs. 5 and 6. Two points are noteworthy. First, the initial data was selected closer to the real parameters for the noisy data match of Fig. 6, and second, the match is more sensitive to the Peclet number for the fracture region than to the α parameter. This is clearly noticed by the big percentage error of the α matched parameter value with respect to the real value, greater than 100%.

Next, results of a radial flow five parameters noisy data match for a layered (horizontal fractures) reservoir, are presented in Fig. 7 and Table 4. The matching parameters used were the fracture dispersivity α, matrix porosity ϕ_2, fracture half-width w, matrix diffusion coefficient D_2, and the dimensionless retardation parameter R. It is important to notice that these matching parameters directly correspond to the real variables of the tracer flow problem, with the exception of the retardation factor R that requires the formation density to estimate the adsorption constant k_d. The finite step injection time considered was t_D=52.5. Results were computed through Eqs. 9 and 12,

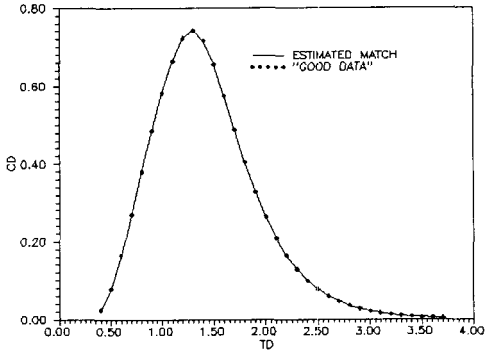

Fig. 5 Tracer response match of "good data" through two parameters, linear flow (vertical fracture).

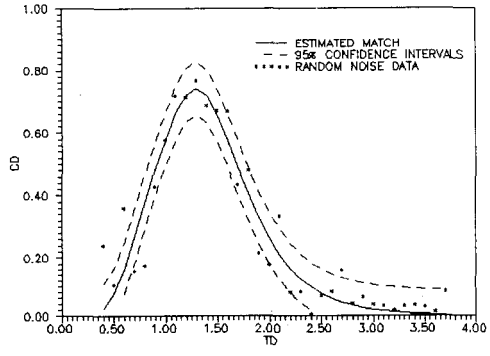

Fig. 6 Random noise tracer response match through two parameters, linear flow (vertical fractures).

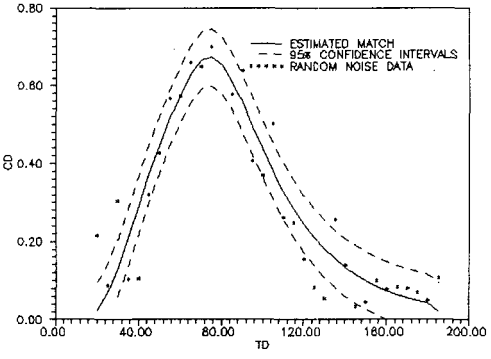

Fig. 7 Random noise tracer response match through five parameters, radial flow for a layered (horizontal fractures) reservoir.

considering only a horizontal fracture, as indicated in Fig. 3, which means that the reservoir thickness h is equal the thickness of the symmetry element E of this figure. The precision used was the same stated previously for the linear flow case, yielding an optimized objective function of 2.362×10^2, with matching parameters reported in Table 4. It can be observed from this figure that despite the dispersion of the noisy data, the match is considered reasonable due to the fact that most of the data fall within the 95% confidence interval bandwidth. For this match results, as also previously pointed out for the linear flow case, and the rest to follow, the fracture dispersivity α was found to be the most sensitive parameter on the inverse solution.

TABLE 4 LAYERED MATRIX-FRACTURE GEOMETRY, FIVE MATCHING PARAMETERS

	Fig. 7	
Real parameters	Initial	Matched
$\alpha_1 = \alpha = 25\,m$	23	25.1672
$\alpha_2 = \phi_2 = 0.01$	.009	0.0128
$\alpha_3 = w = .0001\,m$	0.00008	.000085
$\alpha_4 = D_e = 1.38\text{E-}5m^2/d$	$1E-5$	$1.278E-5$
$\alpha_5 = R$=1.0	.8	.7528

Last, we present results for the cubic block matrix-fracture geometry systems. This geometry is considered a more realistic visualization of a naturally fractured reservoir (Ramírez and Samaniego, 1992). All results are for noisy data matches, presented in Figs. 8-10 and Tables 5-7. The six matching parameters for the general case 3 were those five already mentioned for the layered case, in addition to the matrix block size parameter d, with the same correspondence to real variables and exception previously discussed for the layered case. Cases 1 and 2 are particularizations of case 3, with matching parameters for the former being matrix porosity ϕ_2 and matrix block size d, and for the latter, in addition to these of case 1, the fracture dispersivity α and the fracture half-width w. The finite step injection time considered was t_D=52.5. The original tracer response before being noisly altered, was computed by means of Eqs. 9 and 13. The precision used was the same stated previously for the linear flow case, yielding values of the optimized objective function of approximately 0.02 for cases 1 to 3, with matching parameters reported in Tables 5-7.

TABLE 5 CUBIC BLOCK MATRIX-FRACTURE GEOMETRY, CASE 1, TWO MATCHING PARAMETERS

	Fig. 8	
Real parameters	Initial	Matched
$\alpha_1 = \phi_2 = .01$	0.03	0.0134
$\alpha_2 = d = 2.05m$	1.0	2.29

It can be observed from Figs. 8-10 that despite the dispersion of the noisy data, the match is considered reasonable due to the fact that most of the data fall within the 95% confidence interval bandwidth. Further analysis of these matches based on the results presented in Tables 5-7, indicates important percentage differences of the matched results with respect to the real parameters, with the exception previously mentioned of the fracture dispersivity α, in addition to the retardation factor R.

TABLE 6 CUBIC BLOCK MATRIX-FRACTURE GEOMETRY, CASE 2, FOUR MATCHING PARAMETERS

	Fig. 9	
Real parameters	Initial	Matched
$\alpha_1 = \alpha = 25m$	20	25.35
$\alpha_2 = \phi_2 = .01$	.02	0.045
$\alpha_3 = w = .0001m$	.0015	.00147
$\alpha_4 = d = 2.05m$	.9	1.618

TABLE 7 CUBIC BLOCK MATRIX-FRACTURE GEOMETRY, CASE 3, SIX MATCHING PARAMETERS

	Fig. 10	
Real parameters	Initial	Matched
$\alpha_1 = \alpha = 25\,m$	23	24.867
$\alpha_2 = \phi_2 = 0.01$	.015	0.0153
$\alpha_3 = w = .0001\,m$	0.0001	.000085
$\alpha_4 = d = 2.05\,m$	1.5	2.804
$\alpha_5 = D_e = 1.38\text{E-}5m^2/d$	$9.9E-6$	$9.88E-6$
$\alpha_6 = R$=1.0	.98	.99

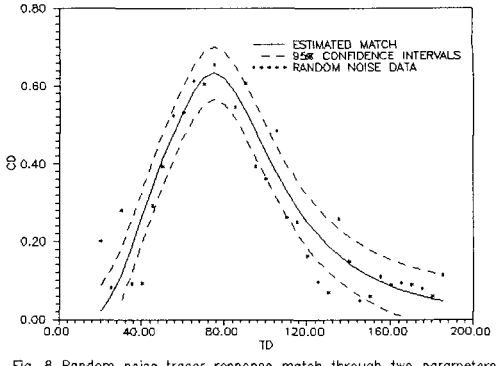

Fig. 8 Random noise tracer response match through two parameters, cubic matrix-fracture geometry.

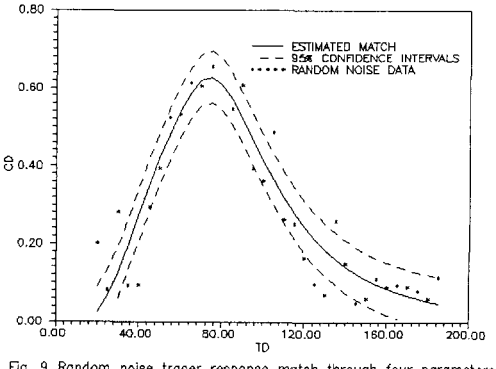

Fig. 9 Random noise tracer response match through four parameters, cubic matrix-fracture geometry.

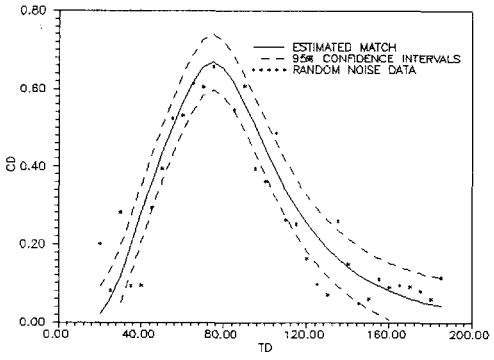

Fig. 10 Random noise tracer response match through six parameters, cubic matrix–fracture geometry

Further match analysis of "good data" results of Fig. 5 and Table 3, and of noisly altered tracer responses of Figs. 6-10 and Tables 4-7, concludes that the percentage errors between the matched and the real parameters values, depend first on the quality of the tracer concentration response, because it has been shown that these errors increase for the latter responses. Based on this finding, it can be stated that for reservoir characterization purposes it is necessary to have data as accurate and representative as possible. Smoothing and filtering data techniques can be used to accomplish this task. Second, results not completely shown in this paper (Ramírez, 1992), indicate that the errors also depend in the closeness of the initial or starting data. Thus, we should follow a synergy oriented interpretation, using information coming from all possible sources, i.e., geological, geophysical, petrophysis, well test analysis, etc.

CONCLUSIONS

The main purpose of this study has been to present a solution for the inverse problem to the flow of tracers in naturally fractured reservoirs. The cases discussed consider mainly radioactive tracers but the solutions used are general, and a particular case would be the flow of chemical tracers.

Based on the material presented in this paper, the following conclusions are pertinent.

1. The Rosenbrock method for nonlinear regression used in this study has proved to be a powerful tool for providing an inverse solution to the flow of tracers.

2. The inverse problem analysis has included the linear flow vertical fractures, and the radial flow cases of horizontal fractures, and cubic block matrix-fracture geometry.

3. The maximum number of possible matching parameters was six, corresponding to the cubic block case.

4. The parameters that showed the most sensitivity on the inverse solutions were the Peclet number for the fracture region P_{e1} for linear flow, and the fracture dispersivity α for the radial cases.

5. The errors between the matched and the real parameters values depend on the quality of the tracer concentration response, and on the closeness of the initial data to the real parameters.

6. A synergy oriented approach should be followed for the interpretation of a tracer test.

NOMENCLATURE

a = advection parameter, Eq. 2, L^2/t
$A_i(x)$ = Airy function
B_1 = function defined by Eq. 7
C = tracer concentration
C_1 = function defined by Eq. 8
$C(t,\alpha_j)$ = calculated tracer concentration
C_D = dimensionless tracer concentration
$\overline{C}_D$ = Laplace space dimensionless .. tracer concentration
C_{Di} = calculated dimensionless tracer concentration .. at t_i
C_{Di} = dimensionless noisy tracer concentration .. at t_i
d = matrix block size, L
d_D = dimensionless matrix block size, .. d / α
D_L = longitudinal dispersion coefficient .. for linear flow, L^2/t
D_2 = matrix diffusion coefficient, L^2/t
D_{D2} = dimensionless matrix diffusion coefficient, .. D_2/a
D_r = longitudinal dispersion coefficient .. for radial flow, L^2/t
E = fracture spacing, L
F = objective function, Eq. 16.
F_1 = function defined by Eq. 4
F_2 = function defined by Eq. 5
h = reservoir thickness, L
k_d = adsorption constant, L^3/M
L = distance from injector to producer, L
ND = number of cubic blocks in reservoir .. thickness h
P_{e1} = Peclet number, dimensionless $v_L L/D_1$
q = constant injection rate, L^3/t
r = radial distance, L
r_D = dimensionless radial distance
r_w = wellbore radius,L
r_{D0} = dimensionless wellbore radius
R = dimensionless parameter, .. $\phi_2/[\phi_2 + \rho k_d(1-\phi_2)]$
s = Laplace space parameter
t = time, t
t_D = dimensionless time, $qt/2\pi h\phi_1\alpha^2$ = .. at/α^2
U = step function, Eq. 3
v = fluid velocity, Eq. 1, L/t
w = fracture half-width, L
x = distance in the x direction, linear flow
x_D = dimensionless distance in the x direction, .. x/L

y = distance in the y direction, linear flow
y_D = dimensionless distance in the y direction, .. y/L
Y = dimensionless parameter defined .. by Eq. 10
Y_0 = dimensionless parameter defined .. by Eq. 11
z = vertical coordinate, radial flow, L
z_{D0} = dimensionless vertical distance of the .. fluid film, $(d/2+\delta)\alpha$

Greek symbols

α = dimensionless parameter, $\phi_2\sqrt{P_{e2}}/(w-\delta)$
α_L = longitudinal fracture dispersivity, L
α_i = dimensionless matching parameters, Eq. 16
β_r = dimensionless parameter, Eq. 15
β_R = constant used to multiply the optimization .. step e when the objective function increases.
γ = dimensionless parameter, $\lambda\alpha^2/a$
δ = stagnant fluid film thickness, L
ε = dimensionless parameter, Eq. 14
λ = radioactive decay constant, $1/t$
ξ = dimensionless parameters, Eqs. 12 and 13
ρ = porous media density, M/L^3
τ = dummy variable of integration, Eq. 3
ϕ = porosity, fraction

Subscripts

c = cubic
D = dimensionless
L = linear
i = initial, index (Eq. 16)
r = radial
0 = origin or related to tracer injection .. concentration
1 = mobile or fractured region
2 = immobile (fluid layer and porous matrix) .. region

REFERENCES

Abramowitz, M. and Stegun, I.A., 1970. Handbook of Mathematical Functions with Formulas, Graphs and Mathematical Tables. National Bureau of Standards, Washington, D.C.

Brigham, W.E. and Abbaszadeh-Dehghani, M., 1987. Tracer Testing for Reservoir Description J. Pet. Tech., Vol. 35, No. 5 (May) 519-527.

Crump, K.S., 1976. Numerical Inversion of Laplace Transforms Using a Fourier Series Approximation. J. ACM, Vol. 23, No. 1 (Jan.) 89-96.

Davis, C.J., 1973. Statistics and Data Analysis in Geology. John Wiley and Sons, New York.

Fossum, M. P. and Horne, R. N., 1982. Interpretation of Tracer Return Profiles at Wairakei Geothermal Field Using Fracture Analysis. Geothermal Resources Counsil, Transactions, Vol. 6.

Fossum, M. P., 1984. Tracer Analysis in a Fractured Geothermal Reservoir: Field Results from Wairakei, New Zealand. Stanford Geothermal Program, SGP-TR-56, Stanford, Ca.

Fuentes-Nucamendi, F.A., 1993. Optimization of Dry Gas Production Systems. M. Sc. report, Department of Petroleum Engineering, Stanford University, Stanford, Ca.

Hensel, W.M., Jr., 1989. A Perspective-Look at Fracture Porosity. SPE Formation Evaluation J., Vol. 4, No. 4 (Dec.) 531-534.

Horne, R.N., and Rodríguez, F., 1983. Dispersion in Tracer Flow in Fractured Geothermal Systems. Geophysical Research Letters, Vol. 10, No. 4, 288-292.

Jensen, C.L., 1983. Matrix Diffusion and Its Effect on the Modeling of Tracer Returns From the Fractured Geothermal Reservoir at Wairakei New Zealand. Stanford Geothermal Program, SGP-TR-71, Stanford, Ca.

Montgomery, D., 1984. Design and Analysis of Experiments. John Wiley and Sons, New York.

O'Hara, H. and Smith, F.J., 1969. The Evaluation of Definite Integrals by Interval Subdivision. Computer Journal, Vol. 12, 179-182.

Pickens, J.F. and Grisak, G.E., 1981. Modeling of Scale-Dependent Dispersion in Hydrogeologic Systems. Water Resour. Res., Vol. 17, No. 6 (Dec.) 1701-1711.

Ramírez, S.J., Rivera, R.J., Samaniego, V.F., and Rodríguez F., 1990. A Semianalytical Solution for Tracer Flow in Naturally Fractured Reservoirs. Proceedings, Fifteenth Workshop on Geothermal Reservoir Engineering, SGP-TR-130, Stanford U., Stanford, Ca., January 23-25.

Ramírez, S.J., Samaniego, V.F., Rivera, R.J., and Rodríguez F., 1991. An Investigation of Radial Tracer Flow in Naturally Fractured Reservoirs Proceedings, Sixteenth Workshop on Geothermal Reservoir Engineering, SGP-TR-134, Stanford U., Stanford, Ca., January 23-25.

Ramírez, S.J., and Samaniego V.F., 1992. A Cubic Matrix-Fracture Geometry Model for Radial Tracer Flow in Naturally Fractured Reservoirs Proceedings, Seventeenth Workshop on Geothermal Reservoir Engineering, SGP-TR-141, Stanford U., Stanford, Ca., January 29-31, 1992.

Ramírez, S.J., 1992 "Flujo de Trazadores en Yacimientos Naturalmente Fracturados", Ph.D dissertation, School of Engineering, National University of Mexico, Nov.

Rosenbrock, H.H., 1960. An Automatic Method for Finding the Greatest or Least Value of a Function. Computer Journal, 3, 175-184.

Shinta, A.A. and Kazemi, H., 1993. Tracer Transport in Characterization of Dual-Porosity Reservoirs. Paper SPE 26636, presented at SPE Annual Technical Conference and Exhibition, Houston, Tx., 3-6 October.

Walkup, G.W., 1984. Characterization of Retention Processes and Their Effect on Analysis of Tracer Tests in Fractured Reservoirs. Stanford Geothermal Program, SGP-TR-77, Stanford, Ca., June.

Walkup, G.W., and Horne, R. N., 1985. Characterization of Tracer Retention Processes and Their Effect on Tracer Transport in Fractured Geothermal Reservoirs. Paper SPE 13610, presented at California Regional Meeting, Bakersfield, Ca., March 27-29.

Weber, K.J. and Baker, M., 1981. Fracture and Vuggy Porosity. Paper SPE 10332, presented at SPE Annual Fall Technical Conference and Exhibition, San Antonio, Tx., 5-7 Oct.